Supplemental Materials

Effects of Long-Term Exercise and a Very High-Fat Diet on Synovial Fluid Metabolomics and Joint Structural Phenotypes in Mice: An Integrated Network Analysis

Alyssa K. Hahn, PhD[1,2,3#], Albert Batushansky, PhD[4#], Rachel A. Rawle, PhD[1,5], Erika Barboza Prado Lopes, PhD[4], Ronald K. June, PhD[1,2,6*] and Timothy M. Griffin, PhD[4,7,8*]

[#]Authors contributed equally to this work

*Co-corresponding authors

Content:

Note: Supplemental Tables S2 and S3 are separate excel file attachments

34

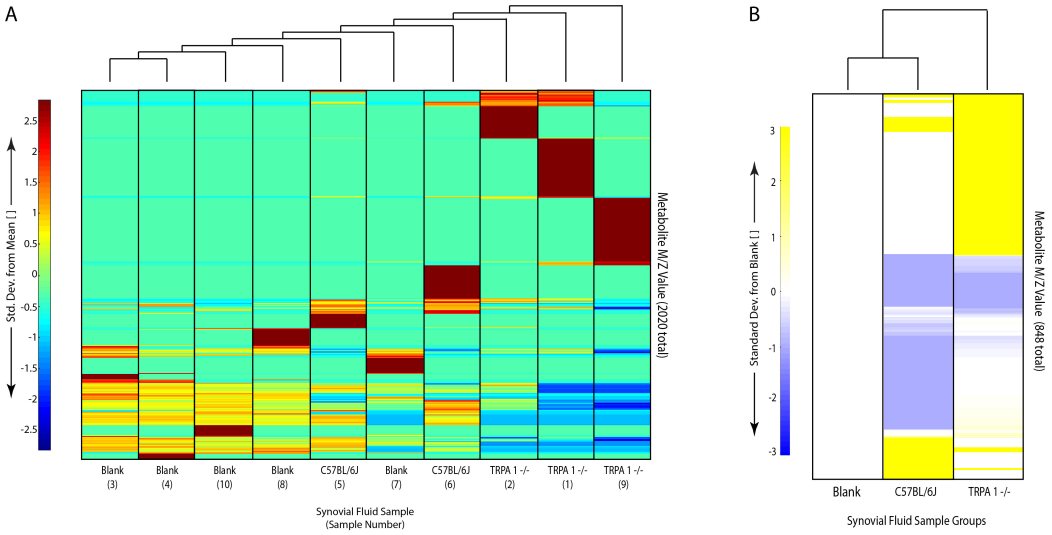

Figure S1: HPLC-MS unsupervised metabolomic analysis of 5 murine SF samples (n=2 C57BL/6J and n=3 TRPA1$^{-/-}$) and 5 blank calcium sodium alginate carrier samples processed in parallel and blinded. A) Heatmap clustergram visualization of unsupervised hierarchical cluster analysis based on median m/z metabolic features. Unblinding sample IDs after cluster analysis showed that individual blank and SF samples clustered separately in all but the position of one sample. B) When metabolite features were averaged by group and normalized to the blank, C57BL/6J and TRPA1$^{-/-}$ mouse samples showed distinct SF metabolomic features, and both groups differed substantially from blank controls.

35

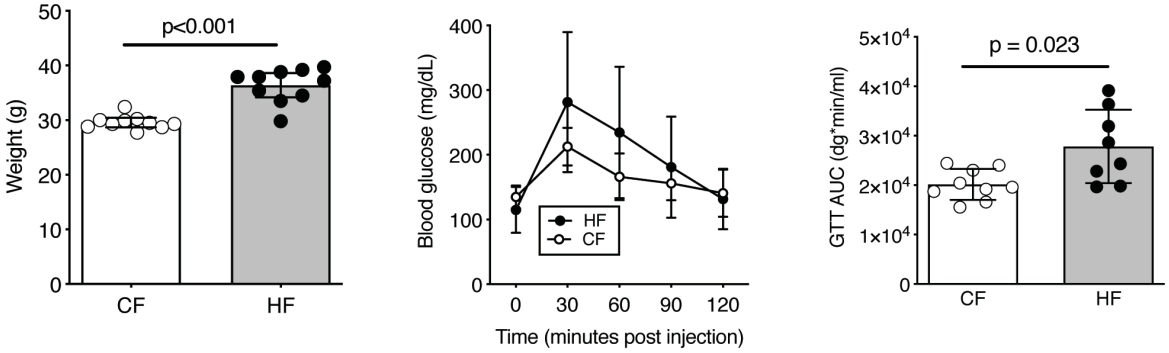

Figure S2: HF diet increased body weight and caused mild glucose intolerance prior to assignment to sedentary or wheel running activity groups. Glucose tolerance testing was performed on a subset of animals at 22 weeks of age, which was 16 weeks after the initiation of HF or CF diet treatments.

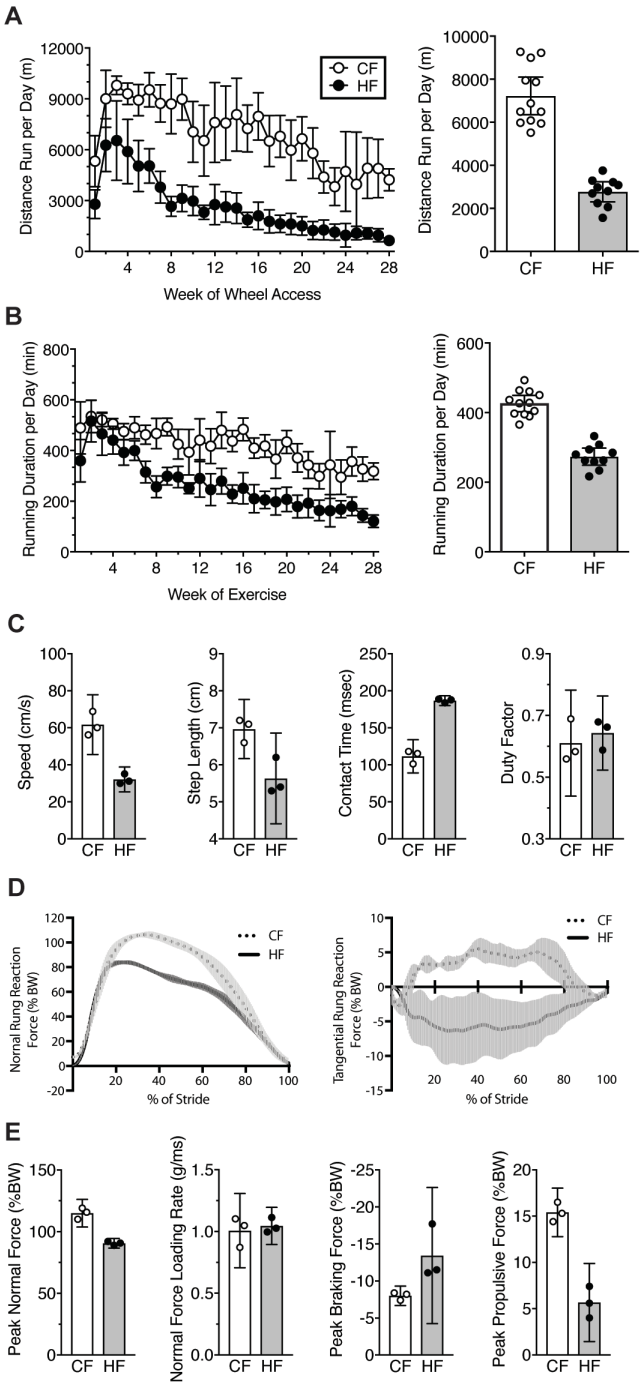

Figure S3. Effect of HF diet on voluntary wheel running behavior and gait biomechanics. A. Average daily running distance decreased significantly with HF diet and age (mean +/- 95%CI). B. Daily running duration also reduced with age, especially in animals fed a HF diet (mean +/- 95% CI). C. After 12 weeks of access to running wheels, animals were housed overnight in a custom force-instrumented running wheel toevaluate the effect of a HF diet on gait kinematicsand kinetics. HF fed animals ran significantly slower with a shorter step length and longercontact time (mean +/- 95% CI). D. HF diet reduced the force impulse of the normal component of the foot-rung reaction force and altered the pattern of tangential force application from primarily propulsive to braking (mean +/- sd). E. HF diet reduced the peak normal force,expressed as percent body weight (BW), but it did not alter the absolute normal force loading rate. HF diet reduced the peak propulsive forces more than the braking forces (mean +/- 95% CI).

66

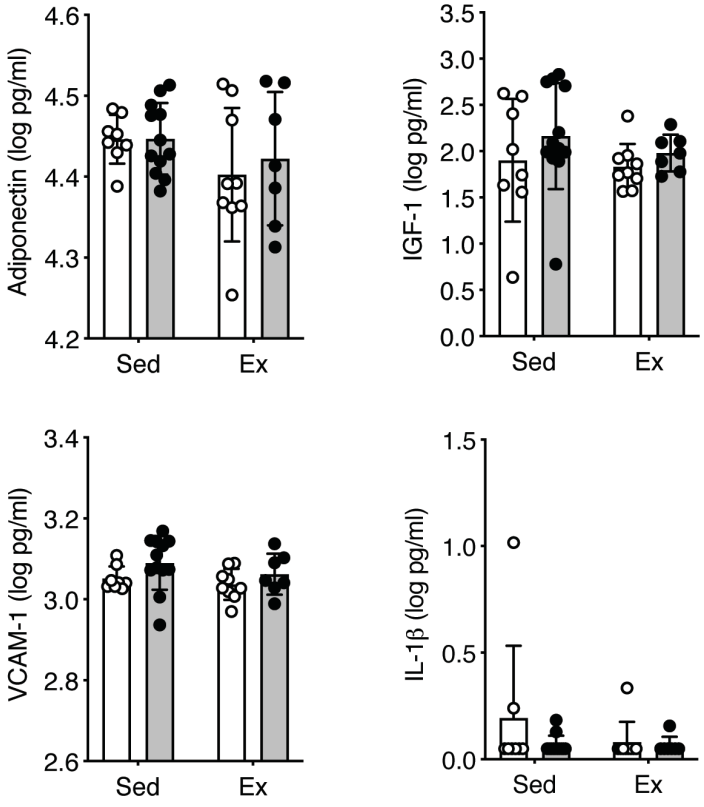

Figure S4: Effect of activity and diet on serum proteins. Serum biomarkers were measured at the study endpoint by luminex and ELISA-based assays. Log-transformed data were analyzed by two-factor analysis of variance, with significance defined as $p<0.05$. No significant effects of activity or diet on these serum biomarkers were detected. For all graphs, values are mean ± s.d.

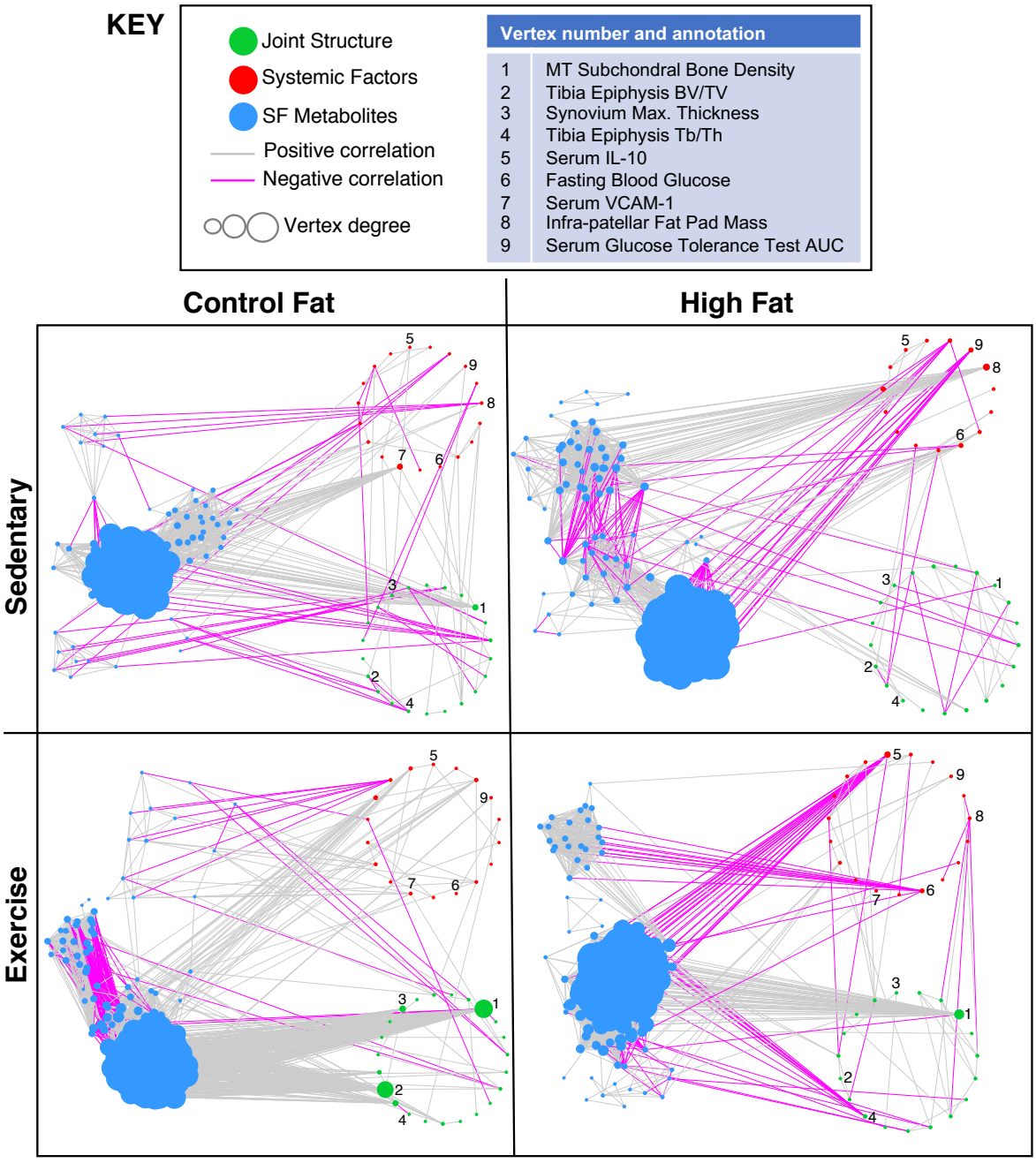

Figure S5: Unabridged correlation-based networks for each diet and physical activity treatment group. Each variable (i.e., "vertex") with ≥1 significant correlation ($r > |\pm 0.5|$ and qFDR < 0.05) is color-coded as indicated in the figure key and grouped accordingly. The number of significant correlations for each vertex (i.e., vertex degree of connectivity) is indicated by the symbol size, and positive and negative correlations between vertices are indicated by line color as shown in the key. The Joint Structure and Systemic Factor variables with the greatest degree of connectivity in a given network are labeled according to vertex number and variable annotation in the key. Note the distinct effects of HF diet and physical activity on the degree of connectivity between systemic versus joint structural factors and SF metabolites. MT: medial tibia; BV/TV: bone volume to total volume; Tb/Th: trabecular thickness; IL-10: interleukin-10; VCAM-1: vascular cell adhesion molecule-1; AUC: area under the curve.

77
78

Table S1. Summary 2-Factor ANOVA Analyses to Evaluate Diet and Activity Effects on Systemic and Joint Structure Outcomes

Figure	Outcome	Log-transformed?	Diet factor (p value)	Activity factor (p value)	Interaction (p value)
2A	Body mass	N	<0.0001	0.0047	0.6887
2A	Body fat	N	<0.0001	<0.0001	0.007
2A	Gondadal Fat Pad mass	N	<0.0001	0.0009	0.0063
2B	Fasting blood glucose	N	0.0015	0.7207	0.101
2B	GTT AUC	N	0.0007	0.9997	0.006
2C	CD45+ PI- cells	N	0.0026	0.5188	0.0295
2C	CD11c+ cells	N	<0.0001	0.0224	0.2939
2C	CD206+ cells	N	<0.0001	0.0395	0.7348
2D	Leptin	Y	<0.0001	0.0044	0.0467
2D	IL-8	Y	0.0045	0.4666	0.5503
2D	CCL2	Y	<0.0001	0.0547	0.6408
2D	IL-10	Y	0.081	0.5944	0.0447
2D	IL-6	Y	0.0619	0.3865	0.4086
2D	IL-12p70	Y	0.7811	0.2925	0.0734
3A	Mod. Mankin OA	N	0.0005	0.9313	0.867
3A	Cartilage Damage	N	0.0003	0.4662	0.7088
3A	Saf-O Loss	N	0.0024	0.8451	0.6704
3A	Tidemark	Y	0.6592	0.3116	0.4976
3A	Hyp. Chondrocytes	N	0.6546	0.0361	0.4591
3A	Osteophyte	N	0.7528	0.0512	0.4465
3B	Max Synovial Thickness	N	0.0617	0.4765	0.8674
3B	Max Synovial Cell Num.	N	0.0188	0.7238	0.1264
3B	IFP mass	N	0.4579	0.2179	0.5842
4A	Subchon. BMD_LT	N	0.1102	0.9903	0.7815
4A	Subchon. BMD_MT	N	0.0011	0.3364	0.8787
4A	Trabecular BMD	N	0.0565	0.5857	0.1753
4B	Trab. BV/TV	N	0.5679	0.5382	0.1814
4B	Trab. Con Den.	N	0.0004	0.601	0.0095
4B	Trab. Thickness	N	0.4498	0.1824	0.0644
4B	Trab. Seperation	N	0.1134	0.3134	0.5763
S2*	Body mass	N	<0.0001		
S2*	GTT AUC	N	0.0234		
S4	Adiponectin	Y	0.6343	0.115	0.6477
S4	IGF-1	Y	0.2165	0.4405	0.7323
S4	VCAM-1	Y	0.0744	0.2264	0.6973
S4	IL-1b	Y	0.2197	0.3208	0.3411
*Two-tailed Student's t-test (pre-exercise analyses)					
	Bonferoni-adjusted p-value threshold (0.05/36):		0.001388889		

Table S4. Network Sensitivity Analysis

Average |r| for the each network

		Random exclusion of 1 sample from each network (iteration #)						
Network	**All Samples**	**#1**	**#2**	**#3**	**#4**	**#5**	**mean**	**stdev**
CS	0.901	0.858	0.931	0.922	0.920	0.925	0.911	0.030
CE	0.917	0.937	0.933	0.933	0.920	0.925	0.930	0.007
HS	0.924	0.938	0.931	0.921	0.931	0.931	0.930	0.006
HE	0.910	0.921	0.919	0.920	0.922	0.926	0.922	0.003

As a test of network robustness, we calculated the average |r| for each network following the random exclusion of 1 sample. This procedure was conducted 5 times for each network.

Table S5: Graph Theory-based Network Properties

Network	Vertices	Edges (neg; %)	Density	Diameter	Transitivity
CF-Sed	304	20778 (216; 1.0)	0.45	13	0.84
CF-Ex	302	18597 (255; 1.4)	0.41	10	0.79
HF-Sed	299	19203 (142; 0.7)	0.43	8	0.85
HF-Ex	301	17786 (106; 0.6)	0.39	12	0.79

Graph theory-based network properties describe the mathematical characteristics of a collection of vertices and the edges that connect those vertices. “Vertices” refers to the number of variables in the network with ≥1 significant correlation, and “Edges” refers the number of significant correlations between all the vertices in the network. Note that nearly all of the Edges are positive correlations. “Density” is the number of actual edges present in the network divided by the number of theoretical potential edges. “Diameter” is the longest of the shortest paths (i.e., minimal number of edges) between any two vertices, and “Transitivity” is the probability to form sub-networks.

Table S6. Group-Specific Coefficient of Variation in Body Composition Outcomes

Group	Body mass	Percent Body Fat	Gonadal Fat Pad Mass	Infrapatellar Fat Pad Mass
CF-Sed	12.8%	15.5%	31.8%	16.3%
CF-Ex	8.2%	15.8%	80.0%	15.3%
HF-Sed	8.7%	4.5%	17.3%	35.7%
HF-Ex	8.9%	6.1%	17.8%	32.4%

Coefficient of variation (CV) was most similar across groups for body mass. Percent body fat CV was reduced with high-fat (HF) diet. In contrast, HF diet increased the CV for infrapatellar fat pad mass. Gonadal fat pad mass CV was most variable among treatment groups, especially due to high variance in CF-Ex mice.

Supplemental Methods

Note: Some sections of the supplemental methods are repeated from the main text to provide context for the additional details.

Animals Treatments and Phenotyping

Mice were housed ≤5 animals per ventilated cage in a temperature-controlled room maintained at 22 ± 3°C on 14/10-hour light/dark cycles with *ad libitum* access to the defined HF or CF diet and water. Although the HF diet used in this study, which is composed of 60% kcal from fat, may not seem clinically relevant, many low-carbohydrate diets (e.g., ketogenic and related diets) exceed this fat content. In addition, the ResearchDiets 60% kcal fat diet used in this study is among the most common diet-induced obesity model systems used in the metabolism field, which is why The Jackson Laboratory has provided it as a commercially available model for over a decade. Thus, there is a large database for comparison and interpretation. Nevertheless, it is important to consider that the use of defined HF diets has limitations and may make it difficult to detect other diet-specific changes (e.g., dietary sugar or fiber) that also contribute to phenotypic outcomes[5].

Animals were weighed weekly and received daily inspection and routine veterinary assessment. At 26 weeks of age, animals not housed with running wheels were single-housed with nestlet and hut enrichment and defined as sedentary. At 24-wks of age, body composition was measured in a subset of 10 CF and 10 HF animals with representative body masses using a dual-energy X-ray absorptiometry (DEXA) system (Lunar PIXImus2; GE LUNAR Corp., USA) followed by pre-exercise glucose tolerance testing as previously described[1]. To understand the effect of diet-induced obesity on limb loading in exercise animals, 3 CF and 3 HF animals were tested after 12 wks of wheel access in a custom-built force-instrumented running wheel to evaluate gait biomechanics as previously described[2]. Between 47-49 wks of age, all animals underwent DEXA scanning and glucose tolerance testing. Following death and blood collection, the epididymal fat pad was collected for isolation and flow cytometry profiling of adipose tissue immune cells as

144 previously described[1]. The infrapatellar fat pad (IFP) was dissected from the left knee
145 following SF collection and weighed.

146

147 *Serum Analysis*

148 1-2 animals from each treatment group were transported to the laboratory for a period of
149 1-2 hours prior to death between 8:30-9:30AM. Animals were killed by rapid decapitation
150 using a small animal rodent guillotine. Blood was collected following decapitation from the
151 carotid arteries and allowed to clot in microvette tubes (CB 300 Z, SARSTEDT, Germany)
152 at room temperature for 20 min and then centrifuged at 10,000g for 5 min. Serum was
153 aliquoted and frozen at -80°C until analysis. Samples were shipped on dry ice to Dr.
154 Virginia Kraus's laboratory at Duke University for analysis. Concentrations of IFN-γ, IL-
155 1β, IL-6, IL-10, IL12p70, IL-8 (KC), and TNF-α were measured using the Mouse Pro-
156 inflammatory Ultra-Sensitive sandwich immunoassay 7-plex kit (#K15012C, MSD, USA).
157 Samples were run undiluted following manufacturer instructions. The lowest levels of
158 detection were 0.33 pg/ml for IFN-γ, 1.12 pg/ml for IL-1β, 20.2 pg/ml for IL-6, 1.98 pg/ml
159 for IL-10, 39.7 pg/ml for IL12p70, 2.58 pg/ml for IL-8, and 0.334 pg/ml for TNF-α. The
160 intra-assay coefficients of variation (CVs) were 3.2% for IFN-γ, 3.2% for IL-1β, 4.7% for
161 IL-6, 4.0% for IL-10, 1.8% for IL12p70, 5.1% for IL-8, and 2.3% for TNF-α. Concentrations
162 of adiponectin were measured in serum diluted 1:1000 following manufacturer
163 instructions (#K0013182, MSD). The lowest level of detection was 0.04 ng/ml, and the
164 intra-assay CV was 5.7%. Concentrations of IGF-1 were measured in serum diluted 1:500
165 following manufacturer instructions (#MG100, R&D, USA). The minimal detectable dose
166 was 3.5 pg/ml, and the intra-assay CV was 2.0%. Concentrations of leptin were measured
167 in serum diluted 1:20 following manufacturer instructions (#MOB00, R&D). The minimal
168 detectable dose was 22 pg/ml, and the intra-assay CV was 3.9 Concentrations of the
169 chemokine CCL2, also known as MCP-1, were measured in serum diluted 1:2 following
170 manufacturer instructions (#MJE00, R&D). The minimal detectable dose was <2 pg/ml,
171 and the intra-assay CV was 4.2%. Concentrations of VCAM-1 were measured in serum

diluted 1:50/1:500 following manufacturer instructions (#MVC00, R&D). The minimal detectable dose was 30 pg/ml, and the intra-assay CV was 2.8%.

Joint Structural Analysis

Following death, the right hind limb was isolated and prepared for high-resolution micro-computed tomography (CT) scanning using a vivaCT 40 scanner (Scanco Medical, Basserdorf, Switzerland) as previously described[3]. Subchondral bone and proximal tibial epiphyseal trabecular bone density and morphology were evaluated following a previous protocol[4]. Joints were trimmed of muscle, rinsed, and decalcified using Cal-Ex™ decalcifying solution (ThermoFisher Scientific, USA) for 3 days at 4°C. Knees were dehydrated in an ethanol gradient and paraffin embedded for sagittal sectioning. Slides were stained with hematoxylin, Fast Green, and Safranin-O for histological grading as described previously[1]. Briefly, two experienced graders evaluated multiple stained sections from the medial and lateral joint compartments. Slides were organized by animal, randomized by treatment, and assigned a temporary identification code to blind graders to group assignment. Each grader independently assigned Modified Mankin OA scores separately for the medial tibia, medial femur, lateral tibia, and lateral femur, with a maximal site-specific score of 24. If needed, divergent scores were re-evaluated and reconciled between graders before averaging the values from each grader and unblinding the sample IDs. Osteophyte severity and synovial pathology were evaluated as previously described[5]. Modified Mankin OA outcomes were previously reported for Sedentary CF and HF animals[1].

Synovial Fluid Metabolomics

SF was collected from the left knee immediately following death using the calcium sodium alginate compound method as previously described[6]. Briefly, the joint capsule was opened superior to the patella with an anterior incision, which was extended medially and

laterally along the patellar tendon to insert a 2 mm diameter Melgisorb wound dressing (Tendra, REF 250600; Goteborg, Sweden) into the joint cavity. The joint was flexed approximately 15 times, and then the SF-soaked Melgisorb was removed and digested in 35 µl of alginate lyase in H_2O (1 unit/mL derived from Flavobacterium, Sigma-Aldrich A1603-100MG) for 30 min at 34°C. 15 µl of 1.0M sodium citrate ($C_6H_5Na_3O_7$) was added prior to freezing at -80°C until metabolomic analysis. Samples were shipped on dry ice to the June Laboratory for further processing. Proteins were precipitated with acetone, and metabolites were extracted using 50:50 water:acetonitrile following previously established protocols[7]. Metabolite extracts were analyzed in positive mode using an Agilent 1290 UPLC system connected to an Agilent 6538 Q-TOF mass spectrometer (Agilent Santa Clara, CA). Metabolites were separated on a Cogent Diamond Hydride hydrophilic interaction chromatography (HILIC) 150 x 2.1 mm column (MicroSolv, Eatontown, NJ) in normal phase using optimized elution methods previously reported [7]. LC-MS data were converted from Agilent's proprietary [.d] files to mzXML files using ProteoWizard's MSConvert program. Mass spectra were then processed using MZMine 2.14 for peak detection, noise threshold (1000), retention time and mass-to-charge (m/z) ratio normalization, and alignment of peaks[8]. Output data contained all detected m/z values and corresponding relative abundance of each m/z value. M/z values are referred to in this study as metabolite features.

Data Analytics and Statistics

Group sample sizes (n=10) were based on variance estimates from previous studies and a desire to detect a 30% difference in the mean modified Mankin OA score due to diet or exercise with ≥80% power at a significance level of p=0.05. Additional animals were included in each group to maintain statistical power in case of unexpected death. However, 3 animals assigned to the exercise cohort in each diet and one HF-sedentary animal died during the course of the experiment due to undetermined causes, resulting in the following final group sizes: CF-Sed (n=12), CF-Ex (n=9), HF-Sed (n=13), HF-Ex (n=9). The sample sizes for some specific outcomes were smaller due to technical

problems and are indicated in the figure legend. Pre-exercise diet treatments were analyzed by two-tailed Student's t-test, and diet and exercise treatment effects were evaluated by two-way ANOVA. Data that did not meet test assumptions for homoscedasticity or normality of residuals were log-transformed. Tests showing a significant effect of diet, exercise, or interaction effects ($p < 0.05$) were followed up with multiple-comparison post-hoc tests to identify individual group differences as specified in figure legends. Statistical tests were conducted using the software Prism 8.4.3 for Mac OS X.

For SF metabolomic analysis, metabolite features with a median intensity value of zero across all experimental groups were removed from the analysis. Remaining intensity values of zeroes were considered below the detection limit and thus replaced with one-half the minimum intensity value identified in the dataset[9]. This resulted in 1.6% of the overall metabolites being replaced with one half the minimum intensity values. Statistical analyses were completed in MATLAB (Mathworks, Inc.) and MetaboAnalyst[9]. Data processing included normalizing by the median, log transformation, and standardization (mean-centered divided by standard deviation) to correct for non-normal distributions. Normalization to the median for each metabolite reduces potential technical variability between samples. Log transformation and standardization enable quantitative comparison of the abundance levels between distinct metabolites. Hierarchical cluster analysis was used as an unsupervised clustering method to illustrate natural clustering of cohorts based on median metabolite intensities for each cohort to visualize the global metabolomic profiles. Differences between cohorts were determined by fold-change analysis (employed prior to normalization) and FDR-corrected two-tailed Student's T-Tests using MetaboAnalyst. These were calculated on raw data before normalization to compare the absolute differences, which can be skewed by normalization. To preserve the magnitude of the differences, fold changes were calculated based on the raw mean metabolite intensities between the control and exercised groups. Two-tailed T-Tests were used to calculate p-values for pairwise comparisons between experimental groups. 2-way ANOVA was not an available option for data analysis in MetaboAnalyst, which prevented us from considering interaction effects in the analysis. Volcano plots show

between-group comparisons of metabolite features, with preliminary discovery cut-off values of p_{FDR} < 0.1 and ≥2 FC. The rationale for the fold change threshold of 2 is that many metabolites are capable of allosteric regulation which has dramatic effects on enzyme activity.

Correlation Network Analysis

Correlation-based networks were constructed for each diet and physical activity condition separately using previously published methods[12]. Data sets for joint structure outcomes (24 variables), systemic metabolic and inflammatory outcomes (19 variables), and SF metabolite levels (264 variables) were obtained for the same animals and integrated (Supplemental Table 1). The number of SF metabolites included in the correlation-based network analyses was obtained after filtering out features with <90% detected values across all samples to avoid artificial correlations that can be caused by high data imputation. Next, individual missing values were imputed using "MICE" (Multivariate Imputation via Chained Equations) package[13] for R-project[14]. MICE performs multiple imputations of missing values based on other observed values, assuming that missing values are random. We used the 'pmm' method that replaces missing values by predictive mean matching based on the other values. The portion of missing values was < 5% of the total sample feature values, and only 1 missing value was imputed per sample feature per experimental group. Activity related data, such as running distance and duration, were excluded from the network analyses to unify the number of starting variables among all four groups. Next, diet- and activity-specific Pearson's correlation matrices were calculated for all samples from each group using the R "psych" package[15]. In parallel, significance tests with FDR correction for MHT for Pearson's r-values were performed. Only correlation coefficients with r>|±0.5| and q_{FDR}<0.05 were considered as significant and used for network construction. We considered Spearman correlations to minimize potential outlier influences, but we considered Pearson's more robust considering that the

metabolomics data were normalized, scaled and transformed. We wanted to avoid another data manipulation (ordering) to decrease the potential for spurious correlations. To minimize the potential effect of outlier-driven correlations on our conclusions, we focused our discussion on robust sub-networks with high connectivity. In addition, the same analysis method was applied to all four groups so that any outlier effects would similarly influence the four networks. We did not conduct any additional multivariate analyses since our goal was to compare networks using a consistent approach rather than attempting to optimize the network model for each condition. To test the robustness of the network, we calculated the average |r| for each network following the random exclusion of 1 sample. This procedure was conducted 5 times for each network. The Table S4 shows minimal changes in |r| for each network, supporting the robustness of the findings.

Networks were visualized in Cytoscape[16]. Graph theory-based network properties and odds ratio analyses were calculated in R using “iGraph” package[17] and built-in functions, respectively. Features that formed sub-networks with high connectivity were tentatively annotated and mapped to metabolic pathways using MetaboAnalyst on-line tools (38) on KEGG data-base[18]. In addition, Dijkstra’s algorithm was used to find the shortest path between body weight and modified Mankin OA score in the network of each diet-activity group. To employ Dijkstra’s algorithm[19], correlation coefficient edge weights were first converted to a distance weights by formula $1-r^2$, where r is a correlation coefficient between any pair of vertices. Next, the Dijkstra’s algorithm was employed using “iGraph” package for R[17]: “all_shortest_paths” function, diameter: “diameter” function, density: “edge_density” function, transitivity: “transitivity” function. The number of vertices and edges (positive and negative) were directly extracted from Cytoscape. The R-code and general workflow for the network construction were performed as previously published[12] Dijkstra’s algorithm can be applied for positive values only. Therefore, the sign of correlation in the network was ignored to calculate the shortest paths, but positive and negative correlations are still indicated in the figure.

Supplemental References

1. Barboza E, Hudson J, Chang W-P, et al. Profibrotic Infrapatellar Fat Pad Remodeling Without M1 Macrophage Polarization Precedes Knee Osteoarthritis in Mice With Diet-Induced Obesity. *Arthritis & Rheumatology*. 2017;69(6):1221-1232. doi:10.1002/art.40056.

2. Roach GC, Edke M, Griffin TM. A novel mouse running wheel that senses individual limb forces: biomechanical validation and in vivo testing. *Journal of Applied Physiology*. 2012;113(4):627-635. doi:10.1152/japplphysiol.00272.2012.

3. Griffin TM, Batushansky A, Hudson J, Lopes EBP. Correlation network analysis shows divergent effects of a long-term, high-fat diet and exercise on early stage osteoarthritis phenotypes in mice. *J Sport Health Sci*. 2020;9(2):119-131. doi:10.1016/j.jshs.2019.05.008.

4. Griffin TM, Huebner JL, Kraus VB, Guilak F. Extreme obesity due to impaired leptin signaling in mice does not cause knee osteoarthritis. *Arthritis Rheum*. 2009;60(10):2935-2944. doi:10.1002/art.24854.

5. Donovan EL, Lopes EBP, Batushansky A, Kinter M, Griffin TM. Independent effects of dietary fat and sucrose content on chondrocyte metabolism and osteoarthritis pathology in mice. *Dis Model Mech*. 2018;11(9):dmm034827. doi:10.1242/dmm.034827.

6. Seifer DR, Furman BD, Guilak F, Olson SA, Brooks SC III, Kraus VB. Novel synovial fluid recovery method allows for quantification of a marker of arthritis in mice. *Osteoarthritis Cartilage*. 2008;16(12):1532-1538. doi:10.1016/j.joca.2008.04.013.

7. Carlson AK, Rawle RA, Adams E, Greenwood MC, Bothner B, June RK. Application of global metabolomic profiling of synovial fluid for osteoarthritis biomarkers. *Biochemical and Biophysical Research Communications*. 2018;499(2):182-188. doi:10.1016/j.bbrc.2018.03.117.

8. Pluskal T, Castillo S, Villar-Briones A, Oresic M. MZmine 2: modular framework for processing, visualizing, and analyzing mass spectrometry-based molecular profile data. *BMC Bioinformatics*. 2010;11:395. doi:10.1186/1471-2105-11-395.

9. Chong J, Soufan O, Li C, et al. MetaboAnalyst 4.0: towards more transparent and integrative metabolomics analysis. *Nucleic Acids Res*. 2018;46(W1):W486-W494. doi:10.1093/nar/gky310.

10. Guijas C, Montenegro-Burke JR, Domingo-Almenara X, et al. METLIN: A Technology Platform for Identifying Knowns and Unknowns. *Anal Chem*. 2018;90(5):3156-3164. doi:10.1021/acs.analchem.7b04424.

11. Li S, Park Y, Duraisingham S, et al. Predicting network activity from high throughput metabolomics. *PLoS Comput Biol*. 2013;9(7):e1003123. doi:10.1371/journal.pcbi.1003123.

12. Batushansky A, Toubiana D, Fait A. Correlation-Based Network Generation, Visualization, and Analysis as a Powerful Tool in Biological Studies: A Case Study in Cancer Cell Metabolism. *BioMed Research International*. 2016;2016:8313272. doi:10.1155/2016/8313272.

13. van Buuren S, Groothuis-Oudshoorn K. mice: Multivariate Imputation by Chained Equations inR. *Journal of Statistical Software*. 2011;45(3). doi:10.18637/jss.v045.i03.

14. Team RC. R: A language and environment for statistical computing. 2014. http://www.R-project.org/.

15. Revelle WR. psych : Procedures for Personality and Psychological Research.

16. Shannon P, Markiel A, Ozier O, et al. Cytoscape: a software environment for integrated models of biomolecular interaction networks. *Genome Res*. 2003;13(11):2498-2504. doi:10.1101/gr.1239303.

17. Csárdi G, Nepusz T. The igraph software package for complex network research. In: *Complex Systems*. 2006; 1695. https://igraph.org.

18. Kanehisa M, Sato Y, Kawashima M, Furumichi M, Tanabe M. KEGG as a reference resource for gene and protein annotation. *Nucleic Acids Res*. 2016;44(D1):D457-D462. doi:10.1093/nar/gkv1070.

19. Dijkstra EW. A note on two problems in connexion with graphs. *Numer Math*. 1959;1(1):269-271. doi:10.1007/BF01386390.